

Dispersal and noise: Various modes of synchrony in ecological oscillators

Paul C. Bressloff & Yi Ming Lai

Journal of Mathematical Biology

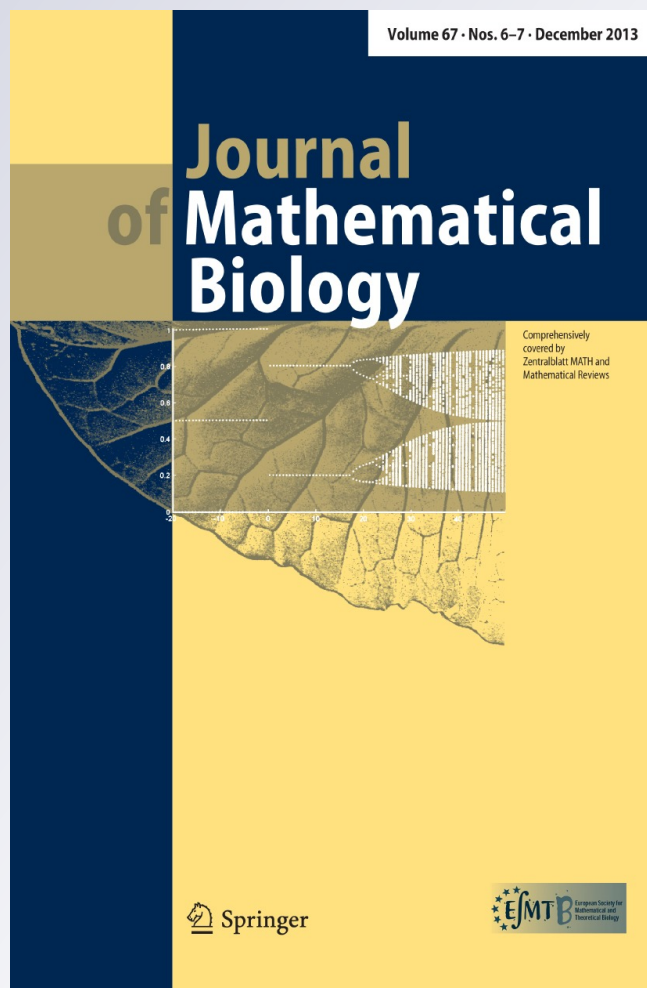
ISSN 0303-6812

Volume 67

Combined 6-7

J. Math. Biol. (2014) 67:1669-1690

DOI 10.1007/s00285-012-0607-9



Your article is protected by copyright and all rights are held exclusively by Springer-Verlag Berlin Heidelberg. This e-offprint is for personal use only and shall not be self-archived in electronic repositories. If you wish to self-archive your article, please use the accepted manuscript version for posting on your own website. You may further deposit the accepted manuscript version in any repository, provided it is only made publicly available 12 months after official publication or later and provided acknowledgement is given to the original source of publication and a link is inserted to the published article on Springer's website. The link must be accompanied by the following text: "The final publication is available at link.springer.com".

Dispersal and noise: Various modes of synchrony in ecological oscillators

Paul C. Bressloff · Yi Ming Lai

Received: 28 March 2012 / Revised: 16 September 2012 / Published online: 21 October 2012
© Springer-Verlag Berlin Heidelberg 2012

Abstract We use the theory of noise-induced phase synchronization to analyze the effects of dispersal on the synchronization of a pair of predator–prey systems within a fluctuating environment (Moran effect). Assuming that each isolated local population acts as a limit cycle oscillator in the deterministic limit, we use phase reduction and averaging methods to derive a Fokker–Planck equation describing the evolution of the probability density for pairwise phase differences between the oscillators. In the case of common environmental noise, the oscillators ultimately synchronize. However the approach to synchrony depends on whether or not dispersal in the absence of noise supports any stable asynchronous states. We also show how the combination of partially correlated noise with dispersal can lead to a multistable steady-state probability density.

Keywords Stochastic population dynamics · Moran effect · Noise-induced synchronization · Predator–prey systems · Metapopulations

Mathematics Subject Classification 92D25 · 60H10

1 Introduction

An important problem in ecology is understanding the mechanisms for synchronizing spatially separated populations or patches that constitute a meta-population. It

P. C. Bressloff (✉)
Department of Mathematics, University of Utah, Salt Lake City,
UT 84112, USA
e-mail: bressloff@maths.ox.ac.uk; bressloff@math.utah.edu

Y. M. Lai
Mathematical Institute, University of Oxford, Oxford, UK
e-mail: lai@maths.ox.ac.uk

is a crucial factor in conservation because synchrony is strongly correlated with the chances of global extinction (Hanski 1998). Conversely, synchrony can help to eliminate an outbreak in pest or pathogen control. For example, work on measles has shown that although vaccination reduces the size of an epidemic, it can also desynchronize populations thus promoting persistence (Earn et al. 1998; Rohani et al. 1999). There are two basic mechanisms for synchronizing patches within a metapopulation (Liebhold et al. 2004): isolated patches can be driven by the same environmental fluctuations (the so-called Moran effect Moran 1953; Hudson and Cattadori 1999) or patches can interact with each other through dispersal in a constant environment (Pecora and Carroll 1998; Jansen and Lloyd 2000; Colombo et al. 2008; Vasseur and Fox 2009). The dominant mechanism will depend on the spatial scale of the metapopulation and the nature of the local patch dynamics. An oscillating patch is often modeled as a limit cycle solution of a system of ordinary differential equations, where the timing along each limit cycle is specified in terms of a single phase variable. The phase-reduction method can then be used to analyze synchronization of an ensemble of oscillators by approximating the high-dimensional limit cycle dynamics as a closed system of equations for the corresponding phase variables (Kuramoto 1984; Ermentrout and Kopell 1991). Within the context of ecology, Goldwyn and Hastings have recently used the theory of weakly coupled phase oscillators to investigate various modes of synchronous and asynchronous phase-locking in predator–prey systems weakly coupled by dispersal (Goldwyn and Hastings 2008, 2009). They have also examined the joint effects of dispersal and environmental fluctuations, by simulating ensembles of predator–prey oscillators with diffusive or global coupling and spatially correlated Poisson inputs (Goldwyn and Hastings 2011); each predator–prey patch is described by the Rosenzweig and MacArthur (RM) model (Rosenzweig and MacArthur 1963; Klausmeier 2010).

Recently, a complementary approach to analyzing the effects of external fluctuations on the synchronization of predator–prey populations has been developed Lai et al. (2011), based on the theory of noise-induced phase synchronization (Pikovsky 1984; Teramae and Tanaka 2004; Goldobin and Pikovsky 2005; Nakao et al. 2007; Marella and Ermentrout 2008; Teramae et al. 2009; Ly and Ermentrout 2009). The latter is an extension of phase-reduction methods to stochastic limit cycle oscillators that provides an analytical framework for studying the synchronisation of an ensemble of oscillators driven by a common randomly fluctuating input; in the case of the Moran effect such an input would be due to environmental fluctuations. Interestingly, noise-induced phase synchronization appears to occur in other areas of biology. For example, evidence for such a mechanism has been found in experimental studies of the olfactory bulb (Galan et al. 2006). It is also suggested by the related phenomenon of spike-time reliability, in which the reproducibility of a single neuron's output spike train across trials is greatly enhanced by a fluctuating input when compared to a constant input (Mainen and Sejnowski 1995; Galan et al. 2008). In our previous work (Lai et al. 2011), we assumed that the predator–prey oscillators were uncoupled (no dispersal). However, we took into account the effects of both correlated and uncorrelated noise sources: environmental fluctuations treated as a common extrinsic noise source, and uncorrelated demographic noise arising from finite size effects. (see Bressloff and Lai 2011 for a related study of noise-induced phase synchronisa-

tion in an ensemble of neural population oscillators). We incorporated demographic noise using a stochastic urn model (McKane and Newman 2004). Approximating the associated master equation using a Kramers–Moyal expansion Gardiner (2009), we then derived a Langevin equation for an ensemble of predator–prey systems. We showed that the multiplicative Gaussian noise terms could be decomposed into a set of independent white noise processes that were uncorrelated across populations (demographic noise), and an additional white noise term that was common to all populations (environmental noise). Assuming that each predator–prey system acted as a limit cycle oscillator in the deterministic limit, we used phase reduction and averaging methods to derive the steady state probability density for pairwise phase differences between oscillators, which was then used to determine the degree of synchronization of the metapopulation.

In this paper, we extend our previous work to the coupled RM model of Goldwyn and Hastings (2011). We show how the theory of stochastic differential equations and noise-induced phase synchronisation can be used to develop an analytical framework for understanding the combined effects of dispersal and noise, at least in the case of two patches. We begin by considering fully correlated environmental noise, that is, a common noise source to both patches (Sect. 2). As previously shown by (Goldwyn and Hastings 2008, 2011), there exist parameter regimes where dispersal alone supports both synchronous and asynchronous phase-locked states. Here we show how the existence of an asynchronous state affects the approach to synchrony when common external fluctuations are included. That is, when dispersal supports only synchronous phase-locking, the time-dependent probability density function (PDF) is unimodal with a width that first increases and then decreases as it moves towards the synchronous state. Moreover, the rate of stochastic synchronization varies approximately linearly with the initial phase difference between the two oscillators. On the other hand, if dispersal also supports asynchronous phase-locking, then for a range of initial conditions the deterministic system converges to the asynchronous state; environmental noise is then required to shift the system out of the basin of attraction of the asynchronous state. This results in a bimodal PDF at intermediate times, before ultimately converging to the synchronous state. Consequently, there is a sharp decrease in the rate of stochastic synchronisation as the initial phase difference increases from zero. We interpret such behaviour in terms of analytical solutions to a Fokker–Planck equation that determines the PDF of the pair-wise phase difference of the oscillators. We then investigate the effects of partially correlated environmental noise on the steady-state PDF, which in the case of common environmental noise reduces to a Dirac delta function at zero phase difference (Sect. 3). In the case where dispersal and common environmental noise both cause synchronous phase-locking, partially correlated noise leads to a unimodal steady-state PDF centered about the synchronous state, which implies that there is a reduction in the degree of synchrony. On the other hand, when dispersal and common environmental noise generate transient peaks at asynchronous states, before eventually converging to the noise-induced synchronous state, the partially correlated noise can cause these transient peaks to become persistent so that the steady-state PDF exhibits multistability.

2 Dispersal and the Moran effect

2.1 The Rosenzweig–MacArthur model

We consider a predator–prey system consisting of N identical patches labeled $i = 1, \dots, N$. In the absence of dispersal or external perturbations, the intrinsic deterministic dynamics of each patch is described by a canonical ecological model known to exhibit limit cycle oscillations, namely, the Rosenzweig–MacArthur (RM) model (Rosenzweig and MacArthur 1963; Klausmeier 2010). For a single isolated patch, the dynamics is given by the pair of equations

$$\frac{dh_i}{dt} = \mu h_i \left(1 - \frac{h_i}{K} \right) - \frac{c a r_i h_i}{b + h_i} \tag{1a}$$

$$\frac{dr_i}{dt} = \frac{a r_i h_i}{b + h_i} - m r_i \tag{1b}$$

where h_i represents the population of prey (or herbivores) and r_i the population of predators. The RM model assumes logistic growth of prey with rate μ up to a carrying capacity K , linear predator mortality of rate m , and a Holling type-II (or Michaelis–Menten) functional response with parameters a, b . The loss of prey due to predation also depends linearly on c with $c > 1$, which implies that the loss in prey population due to predation is faster than the gain in predators. Equation (1) can be nondimensionalised as in Goldwyn and Hastings (2008) to obtain, for the i -th population:

$$\frac{dh_i}{d\tau} = \frac{1}{\epsilon} \left(h_i(1 - \alpha h_i) - \frac{r_i h_i}{1 + h_i} \right) \equiv F_h(h_i, r_i) \tag{2a}$$

$$\frac{dr_i}{d\tau} = \frac{r_i h_i}{1 + h_i} - \eta r_i \equiv F_r(h_i, r_i) \tag{2b}$$

Here $\tau = at, \alpha = b/K, \eta = m/a, \epsilon = a/\mu$ and we have rescaled the populations according to $h_i \rightarrow h_i/b, r_i \rightarrow (ac/\mu b)r_i$. The pair of equations (2) can be rewritten in the vector form

$$\frac{d\mathbf{x}_i}{dt} = \mathbf{F}(\mathbf{x}_i) \tag{3}$$

where $\mathbf{x}_i = (h_i, r_i)^T$ and $\mathbf{F} = (F_h, F_r)^T$. It has previously been shown that $\alpha < 1$ and $\eta < (1 - \alpha)/(1 + \alpha)$ is a parameter regime where stable limit cycles exist (Hastings 1997). Two examples of deterministic limit cycles are shown in Fig. 1.

Migration of the predator and prey species between patches is represented by the per capita rates D_h and D_p and the symmetric connectivity matrix C_{ij} . The component $C_{ij} = 1$ if there is mutual migration between the i -th and j -th patch, and $C_{ij} = 0$ otherwise. The Moran effect is modeled by assuming that all of the predator populations and all of the prey populations are driven by a common white noise term $\eta(t)$. That is, $\eta(t)$ is described by zero mean Gaussian processes with two-point correlation

$$\langle \eta(t)\eta(t') \rangle = \delta(t - t'), \tag{4}$$

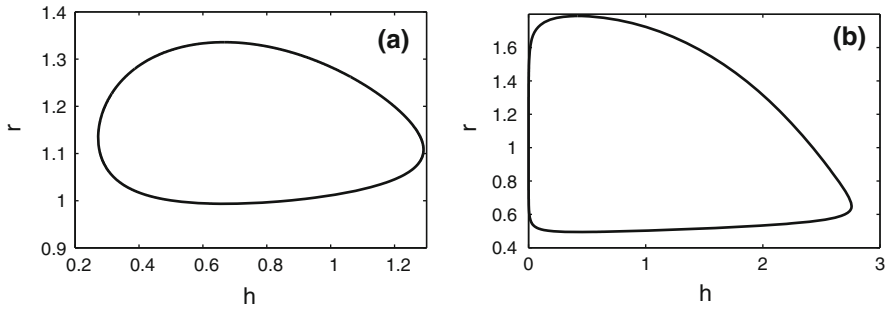


Fig. 1 Limit cycles in the h - r plane for an isolated RM patch. **a** $\epsilon = 0.1, \alpha = 0.4, \eta = 0.4$. **b** $\epsilon = 0.1, \alpha = 0.3, \eta = 0.3$

where $\delta(t)$ denotes the Dirac delta function. From now on we set $D_h = D_p = D$ with D a small parameter in order to simplify the analysis. Also, taking the strength of the extrinsic noise to be scaled by a small parameter σ , we obtain the following system of Langevin equations for the stochastic population variables $\mathbf{X}_i = (H_i, R_i)^T$:

$$\frac{dH_i}{d\tau} = F_h(\mathbf{X}_i) + D \sum_{j=1}^N C_{ij}(H_j - H_i) + \sigma H_i \eta(t) \tag{5a}$$

$$\frac{dR_i}{d\tau} = F_r(\mathbf{X}_i) + D \sum_{j=1}^N C_{ij}(R_j - R_i) + \sigma R_i \eta(t). \tag{5b}$$

Note that we have followed standard treatments of environmental noise by assuming that environmental fluctuations are proportional to population size (Turelli 1978; Oksendal 2000). Moreover, the resulting multiplicative terms are usually interpreted in the Ito sense.

2.2 Phase reduction and averaging

Suppose that in the absence of dispersal and external noise, each patch acts dynamically as a limit cycle oscillator. Following previous studies of noise-induced phase synchronization (Pikovsky 1984; Teramae and Tanaka 2004; Goldobin and Pikovsky 2005; Teramae et al. 2009; Ly and Ermentrout 2009; Lai et al. 2011), we introduce a single scalar variable $\theta_i \in [0, 2\pi)$ that represents the phase of the i -th oscillator. That is, each isolated limit cycle evolves according to the simple phase equation $\dot{\theta}_i = \omega$, where ω is the natural frequency of the oscillator and the phase-plane representation of the limit cycle is $\mathbf{x}_i^*(t) = \mathbf{x}^*(\theta_i(t))$. The notion of phase is then extended into some neighborhood $\mathcal{M} \in \mathbb{R}^2$ of the i -th limit cycle using an isochronal mapping $\Pi : \mathcal{M} \rightarrow [0, 2\pi)$ with $\theta_i = \Pi(\mathbf{x}_i)$. Assuming that the limit cycle is sufficiently attracting in the presence of weak dispersal and noise, the dynamics can be restricted to the neighborhood \mathcal{M} with high probability. This allows us to define a stochastic phase variable for each oscillator according to $\Theta_i = \Pi(\mathbf{X}_i)$ with \mathbf{X}_i evolving according

to the Langevin equation (5). Moreover, the standard deterministic phase reduction method used in (Goldwyn and Hastings 2008, 2009) can be extended to the Langevin equation (5), provided that the multiplicative noise is first converted to Stratonovich form (Gardiner 2009). Carrying out the phase reduction then leads to the following stochastic differential equation (SDE) for the stochastic phase variables $\Theta_i(t)$ (Teramae and Tanaka 2004; Nakao et al. 2007; Teramae et al. 2009):

$$d\Theta_i = \left(\omega + D\mathbf{Z}(\Theta_i) \cdot \sum_{j=1}^N C_{ij} \begin{pmatrix} H(\Theta_j) - H(\Theta_i) \\ R(\Theta_j) - R(\Theta_i) \end{pmatrix} - \frac{\sigma^2}{2} \mathbf{Z}(\Theta_i) \cdot \begin{pmatrix} H(\Theta_i) \\ R(\Theta_i) \end{pmatrix} \right) dt + \sigma \left[\mathbf{Z}(\Theta_i) \cdot \begin{pmatrix} H(\Theta_i) \\ R(\Theta_i) \end{pmatrix} \right] dW(t), \tag{6}$$

where $dW = \eta(t)dt$ and

$$\langle dW(t) \rangle = 0, \quad \langle dW(t)dW(t) \rangle = dt. \tag{7}$$

Here $\mathbf{Z} = (Z_h, Z_p)$ is the infinitesimal phase resetting curve (PRC) whose components are defined according to

$$Z_k(\theta) \equiv \frac{\partial}{\partial x_k} \Pi \Big|_{\mathbf{x}=\mathbf{x}^*(\theta)}, \quad k = h, r \tag{8}$$

such that $\sum_k Z_k(\theta) F_k(\mathbf{x}^*(\theta)) = \omega$. Note that all terms multiplying the PRC in Eq. (6) are evaluated on the limit cycle so that, for example, $H(\Theta_j) = H_j(\mathbf{x}^*(\Theta_j))$. It can be shown that the PRC is the unique 2π -periodic solution of the adjoint linear equation (Ermentrout and Kopell 1991)

$$\frac{dZ_k}{dt} = - \sum_{j=h,r} (\mathbf{x}^*(t)) Z_j(t), \tag{9}$$

where $F_{jk} = \partial F_j / \partial x_k$. The PRC can be evaluated numerically by solving the adjoint equation backwards in time, since all non-zero Floquet exponents of solutions to the adjoint equation have positive real part. The $\mathcal{O}(\sigma^2)$ correction to the natural frequency is a consequence of the conversion from Ito to Stratonovich noise (Gardiner 2009).

In order to simplify the analysis of noise-induced synchronization, we now convert Eq. (6) from a Stratonovich to an Ito system of Langevin equations:

$$d\Theta_i = \mathcal{A}_i(\Theta)dt + d\zeta_i(\Theta_i, t), \tag{10}$$

where $\{\zeta_i(\Theta_i, t)\}$ are correlated Wiener processes and $\Theta = (\Theta_1, \dots, \Theta_N)$. That is,

$$d\zeta_i(\Theta_i, t) = \sigma \alpha(\Theta_i) dW(t), \tag{11}$$

with

$$\alpha(s) = \mathbf{Z}(s) \cdot \begin{pmatrix} H(s) \\ P(s) \end{pmatrix} \tag{12}$$

such that

$$\langle d\zeta_i(\Theta_i, t) \rangle = 0, \quad \langle d\zeta_i(\Theta_i, t)d\zeta_j(\Theta_j, t) \rangle = \Delta_{ij}(\Theta)dt. \tag{13}$$

Here $\Delta_{ij}(\Theta)$ is the equal-time correlation matrix

$$\Delta_{ij}(\Theta) = \sigma^2\alpha(\Theta_i)\alpha(\Theta_j). \tag{14}$$

The drift term $\mathcal{A}_i(\Theta)$ is given by

$$\mathcal{A}_i(\Theta) = \omega + \frac{\sigma^2}{2}\alpha(\Theta_i)\partial_{\Theta_i}\alpha(\Theta_i) - \frac{\sigma^2}{2}\alpha(\Theta_i) + D\mathbf{Z}(\Theta_i) \cdot \sum_{j=1}^N C_{ij}\mathbf{R}(\Theta_i, \Theta_j), \tag{15}$$

where we have set

$$\begin{pmatrix} H(\Theta_j) - H(\Theta_i) \\ R(\Theta_j) - R(\Theta_i) \end{pmatrix} := \mathbf{R}(\Theta_i, \Theta_j). \tag{16}$$

It follows that the ensemble is described by a multivariate Fokker–Planck equation of the form

$$\frac{\partial P(\boldsymbol{\theta}, t)}{\partial t} = - \sum_{i=1}^N \frac{\partial}{\partial \theta_i} [\mathcal{A}_i(\boldsymbol{\theta})P(\boldsymbol{\theta}, t)] + \frac{1}{2} \sum_{i,j=1}^N \frac{\partial^2}{\partial \theta_i \partial \theta_j} [\Delta_{ij}(\boldsymbol{\theta})P(\boldsymbol{\theta}, t)]. \tag{17}$$

As first shown by [Yoshimura and Arai \(2008\)](#), and further developed by [Teramae et al. \(2009\)](#), considerable care must be taken in carrying out the phase reduction procedure in the presence of Gaussian white noise in order to obtain the correct form of the drift terms $\mathcal{A}_i(\Theta)$. However, the correction terms derived in [Teramae et al. \(2009\)](#) are not required provided that the limit cycles are sufficiently strongly attracting. Even if this is not the case, neglecting such terms does not affect our subsequent analysis.

Having obtained the FP equation (17), we can now carry out the averaging procedure of [Nakao et al. \(2007\)](#), see also [Ly and Ermentrout \(2009\)](#). The basic idea is to introduce the slow phase variables $\boldsymbol{\psi} = (\psi_1, \dots, \psi_N)$ according to $\theta_i = \omega t + \psi_i$ and set $Q(\boldsymbol{\psi}, t) = P(\{\omega t + \theta_i\}, t)$. For sufficiently small D and σ , Q is a slowly varying function of time so that we can average the Fokker–Planck equation for Q over one cycle of length $T = 2\pi/\omega$. The averaged FP equation for Q is thus ([Nakao et al. 2007](#))

$$\frac{\partial Q(\boldsymbol{\psi}, t)}{\partial t} = - \sum_{i=1}^N \frac{\partial}{\partial \psi_i} [\bar{\mathcal{A}}_i(\boldsymbol{\psi})Q(\boldsymbol{\psi}, t)] + \frac{1}{2} \sum_{i,j=1}^N \frac{\partial^2}{\partial \psi_i \partial \psi_j} [\bar{\Delta}_{ij}(\boldsymbol{\psi})Q(\boldsymbol{\psi}, t)], \tag{18}$$

where

$$\begin{aligned}
 \bar{\mathcal{A}}_i &= \frac{1}{T} \int_0^T \mathcal{A}_i(\omega t + \psi_1, \dots, \omega t + \psi_N) dt - \omega, \\
 &= \frac{D}{T} \int_0^T \mathbf{Z}(\omega t + \psi_i) \cdot \sum_{j=1}^N C_{ij} \mathbf{R}(\omega t + \psi_i, \omega t + \psi_j) dt \\
 &\quad + \frac{\sigma^2}{2T} \int_0^T [\alpha(\omega t + \psi_i) \partial_{\psi_i} \alpha(\omega t + \psi_i)] dt - \frac{\sigma^2}{2T} \int_0^T \alpha(\omega t + \psi_i) dt \\
 &= D \sum_{j=1}^N C_{ij} \mathcal{H}(\psi_j - \psi_i) - \frac{\sigma^2}{2} \bar{\alpha}
 \end{aligned} \tag{19}$$

since $[\alpha(\omega t + \psi_i)^2]_0^T = 0$, and

$$\begin{aligned}
 \bar{\Delta}_{ij}(\boldsymbol{\psi}) &= \frac{1}{T} \int_0^T \Delta_{ij}(\omega t + \psi_1, \dots, \omega t + \psi_N) dt \\
 &= \frac{\sigma^2}{T} \int_0^T \alpha(\omega t + \psi_i) \alpha(\omega t + \psi_j) dt \\
 &= \sigma^2 \Delta(\psi_j - \psi_i)
 \end{aligned} \tag{20}$$

with

$$\mathcal{H}(\psi) = \frac{1}{T} \int_0^T \mathbf{Z}(\omega t) \cdot \mathbf{R}(\omega t, \omega t + \psi) dt \tag{21}$$

and

$$\Delta(\psi) = \frac{1}{T} \int_0^T \alpha(\omega t) \alpha(\omega t + \psi) dt. \tag{22}$$

The averaged FP equation has a corresponding SDE that describes the evolution of the stochastic phases $\Psi_i(t)$:

$$d\Psi_i = \left(D \sum_{j=1}^N C_{ij} \mathcal{H}(\Psi_j - \Psi_i) - \frac{\sigma^2}{2} \bar{\alpha} \right) dt + d\bar{\zeta}_i(\boldsymbol{\Psi}, t) \tag{23}$$

with

$$\langle d\bar{\zeta}_i(\boldsymbol{\Psi}, t) \rangle = 0, \quad \langle d\bar{\zeta}_i(\boldsymbol{\Psi}, t) d\bar{\zeta}_j(\boldsymbol{\Psi}, t) \rangle = \bar{\Delta}_{ij}(\boldsymbol{\Psi}) dt. \tag{24}$$

2.3 Results for a pair of oscillators

Let us now focus on a pair of oscillators ($N = 2$) with $C_{12} = C_{21} = 1$, and define the phase difference $\Phi = \Psi_2 - \Psi_1$. The averaged SDE (23) reduces to the pair of equations

$$d\Psi_1 = \left(D\mathcal{H}(\Phi) - \frac{\sigma^2}{2}\bar{\alpha} \right) dt + d\bar{\zeta}_1(\Phi, t) \tag{25a}$$

$$d\Psi_2 = \left(D\mathcal{H}(-\Phi) - \frac{\sigma^2}{2}\bar{\alpha} \right) dt + d\bar{\zeta}_2(\Phi, t), \tag{25b}$$

with

$$\begin{aligned} \langle d\bar{\zeta}_1(\Phi, t)d\bar{\zeta}_1(\Phi, t) \rangle &= \langle d\bar{\zeta}_2(\Phi, t)d\bar{\zeta}_2(\Phi, t) \rangle = \sigma^2 \Delta(0) \\ \langle d\bar{\zeta}_1(\Phi, t)d\bar{\zeta}_2(\Phi, t) \rangle &= \langle d\bar{\zeta}_2(\Phi, t)d\bar{\zeta}_1(\Phi, t) \rangle = \sigma^2 \Delta(\Phi) \end{aligned} \tag{26}$$

Taking the difference of the equations (25) and using the result that the difference between two Gaussian random variables is also Gaussian leads to the scalar SDE

$$d\Phi = DG(\Phi)dt + \sigma K(\Phi)dW(t), \tag{27}$$

where $G(\phi) = \mathcal{H}(\phi) - \mathcal{H}(-\phi)$ is the odd part of the phase interaction function \mathcal{H} , $W(t)$ is a Wiener process and

$$\begin{aligned} K(\Phi) &= \frac{1}{\sigma} \sqrt{\langle [d\bar{\zeta}_2(\Phi, t) - d\bar{\zeta}_1(\Phi, t)][d\bar{\zeta}_2(\Phi, t) - d\bar{\zeta}_1(\Phi, t)] \rangle} \\ &= \sqrt{2[\Delta(0) - \Delta(\Phi)]}. \end{aligned} \tag{28}$$

In the absence of extrinsic noise, the dynamics of the phase difference ϕ is given by the deterministic differential equation (Ermentrout and Kopell 1991; Goldwyn and Hastings 2008)

$$\frac{d\phi}{dt} = DG(\phi), \tag{29}$$

Conditions for synchrony are then determined entirely by the function G , which itself depends on the PRC and the nature of the diffusive coupling. The steady or phase-locked states are given by the zeros of G , $G(\phi) = 0$, and are stable when $G'(\phi) < 0$ and unstable when $G'(\phi) > 0$. The rate of convergence to a given steady state is determined by the magnitude of $G'(\phi)$ at that point. In Fig. 2, we plot $G(\phi)$ for the same two sets of parameters used in Fig. 1. In Fig. 2a the synchronous state $\phi = 0$ is the only stable steady state, whereas in Fig. 2b there are additional stable asynchronous states at $\phi \approx 1.78$ (and by symmetry $\phi \approx 2\pi - 1.78$); the asynchronous states have a much larger basin of attraction compared to the synchronous state. When noise

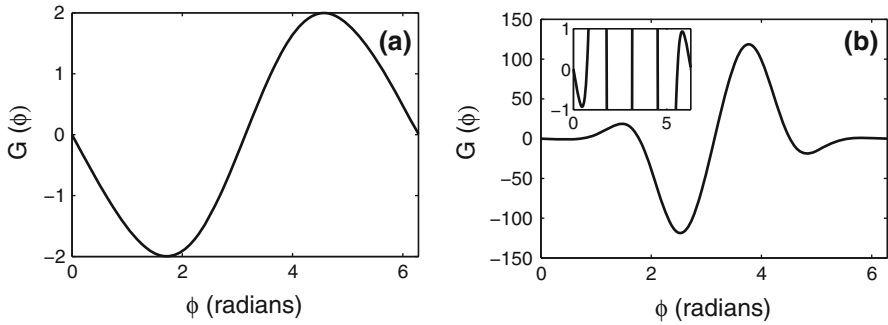


Fig. 2 Numerically evaluated G-functions. **a** $\epsilon = 0.1, \alpha = 0.4, \eta = 0.4$. Only stable phase-locked state is the synchronous state $\phi = 0$. **b** $\epsilon = 0.1, \alpha = 0.3, \eta = 0.3$. There is now an additional pair of stable asynchronous states. *Inset* close-up of behaviour near $\phi = 0$

is included, the stochastic phase difference evolves according to the SDE (52) with corresponding FP equation of the form

$$\frac{\partial P(\phi, t)}{\partial t} = -D \frac{\partial}{\partial \phi} G(\phi) P(\phi, t) + \frac{\sigma^2}{2} \frac{\partial^2}{\partial \phi^2} K(\phi)^2 P(\phi, t). \tag{30}$$

The steady-state solution P_0 satisfies the equation

$$G(\phi) P_0(\phi) = \frac{\sigma^2}{2D} \frac{d}{d\phi} K(\phi)^2 P_0(\phi), \tag{31}$$

which implies that

$$K(\phi)^2 P_0(\phi) = A \exp\left(\int_0^\phi \frac{2DG(\theta)}{\sigma^2 K^2(\theta)} d\theta\right), \tag{32}$$

where A is a normalization factor such that $\int_0^{2\pi} P_0(\phi) d\phi = 1$. Figure 3 shows that the K -function has zeros at $\phi = 0 = 2\pi$, suggesting that the steady-state PDF $P_0(\phi)$ blows up at $\phi = 0$, that is, $P_0(\phi) = \delta(\phi)$. This implies that the common noise source causes total synchronization in the limit $t \rightarrow \infty$.

In order to look at transient behavior, we solve the FP equation (30) numerically assuming the initial condition $P(\phi, 0) = \delta(\phi - \phi_0)$. The results are shown in Fig 4a for the first parameter set of Figs. 1, 2 and 3, for which there are no asynchronous phase-locked states. The initial delta function at $\phi = \phi_0 \neq 0$ first broadens as it moves towards the steady state at $\phi = 0$, and then narrows again as it tends towards a delta function centered at $\phi = 0$, indicating complete phase synchronization. In Fig. 4b we plot the time evolution of one measure of the degree of synchrony $\Pi_0(t)$, namely, $\Pi_0(t) = \int_{-\Delta\phi}^{\Delta\phi} P(\phi, t) d\phi$. That is, $\Pi_0(t)$ is the probability that at time t the phase difference ϕ is within $\Delta\phi$ radians of the synchronous state $\phi = 0$. For concreteness we take $\Delta\phi = 0.2$, although the results do not depend on the precise choice for $\Delta\phi$ provided $\Delta\phi \ll \pi$. For the second parameter set of Figs. 1, 2 and 3, for which the

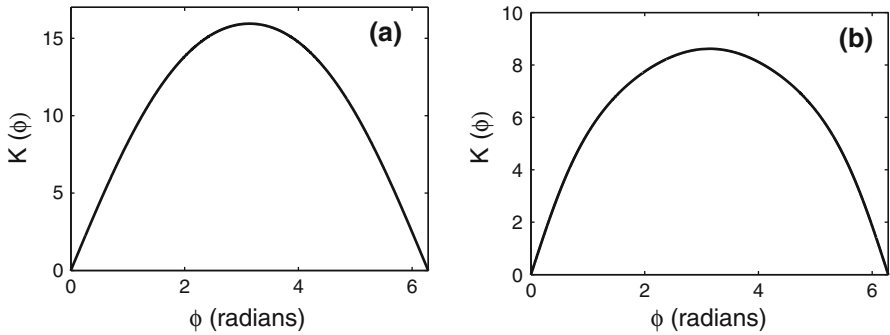


Fig. 3 Numerically evaluated K-functions. *Left a* $\epsilon = 0.1, \alpha = 0.4, \eta = 0.4$. *b* $\epsilon = 0.1, \alpha = 0.3, \eta = 0.3$

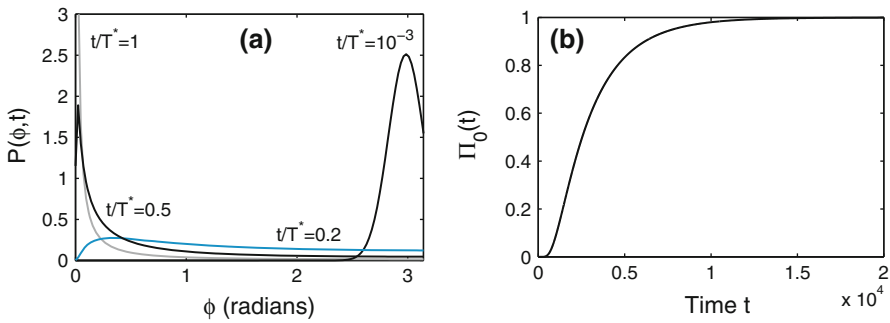


Fig. 4 Monostable case: $\epsilon = 0.1, \alpha = 0.4, \eta = 0.4$ with dispersal coefficient $D = 10^{-4}$ and $\sigma = 5 \times 10^{-3}$. The initial condition is a delta function $\delta(\phi - \phi_0)$ with $\phi_0 = 3$ radians. **a** The PDF $P(\phi, t)$ is plotted as a function of ϕ at several points in time t , normalised with respect to the time T^* taken to synchrony (the peak at $t/T^* = 1$ is not shown here as it would distort the scale of the figure). Synchrony here is defined as when $\Pi_0(t) = \int_{-0.2}^{0.2} P(\phi, t) d\phi > 0.75$, which yields $T^* = 4090$. **b** Plot of $\Pi_0(t)$ against time

synchronous state coexists with a pair of stable asynchronous states, the temporal evolution of the PDF is very different. In particular, if the initial phase is within the basin of attraction of the asynchronous state $\phi = \phi_a \approx 1.78$ in the absence of noise, then the corresponding PDF develops a bimodal structure at intermediate times before moving towards $\phi = 0$ and eventually converging to the expected delta function, see Fig. 5a. The approach to synchrony is significantly slower as shown in Fig. 5b. In Fig. 6a we directly compare the two cases by determining how the time to synchrony T varies with the initial phase ϕ_0 . In order to make the comparison, we normalize time with respect to the total time to synchrony T^* . In the absence of an asynchronous state, T varies relatively slowly with ϕ_0 . On the other hand, T is a step-like function of ϕ_0 in the presence of the asynchronous state ϕ_a . The presence or absence of an asynchronous state can also be discerned by plotting the probability density $P(\phi_a, t)$ as a function of time, see Fig. 6b. It can be seen that the probability density is much less in the monostable case, with the low peak simply reflecting the transient passage to the synchronous state. In Fig. 6a we also show data points based on direct numerical simulations of the SDE model for the phase difference (52). It can be seen that there

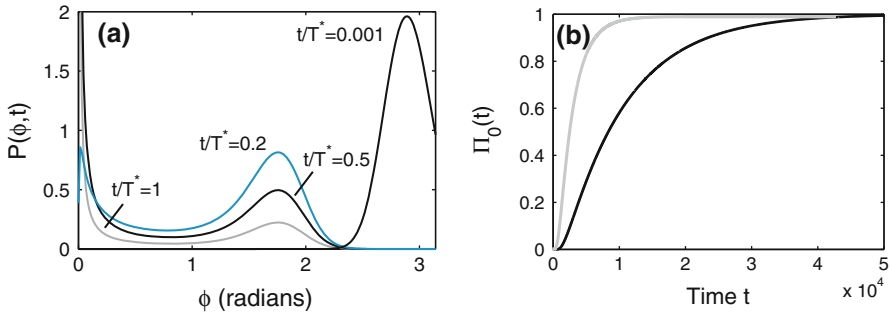


Fig. 5 Multistable case: $\epsilon = 0.1$, $\alpha = 0.3$, $\eta = 0.3$ with dispersal $D = 10^{-4}$ and $\sigma = 5 \times 10^{-3}$. The initial condition is a delta function $\delta(\phi - \phi_0)$ with $\phi_0 = 3$ radians. **a** The PDF $P(\phi, t)$ is plotted as a function of ϕ at several points in time t normalised with respect to the time T^* taken to synchrony. Synchrony is defined as in Fig. 4 but now $T^* = 14, 825$. **b** Plot of $\Pi_0(t)$ against time (corresponding curve from Fig. 4b is shown in gray)

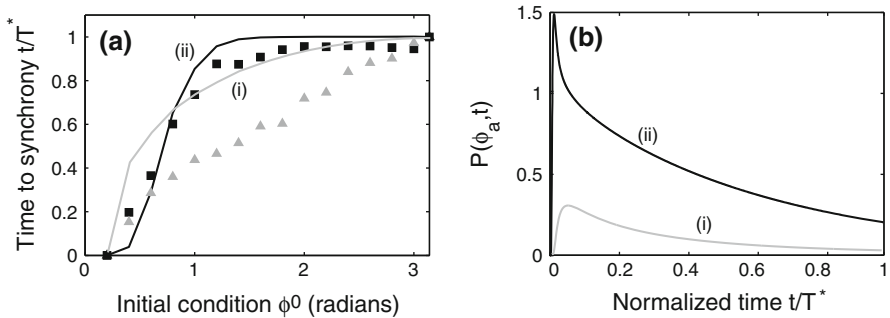


Fig. 6 Comparison of (i) monostable and (ii) multistable cases. **a** Plots of time taken to synchrony T (normalized with respect to $T^* = T(\phi_0 = 3)$) as a function of the initial condition ϕ_0 . Continuous curves are based on solutions to the FP equation (30). Data points are based on numerical solutions of the SDE (52). **b** Plot of the PDF $P(\phi, t)$ at the asynchronous state $\phi_a \approx 1.78$

is good agreement between the FP equation and the SDE in the multistable case. The latter is less accurate in the monostable case but the basic trend is still captured. Note that one source of error is that the criterion for synchrony in the FP equation and the SDE are different. In the former case, we define the time to synchrony to be when $\Pi_0(t) = \int_{-0.2}^{0.2} p(\phi, t) d\phi > 0.75$. On the other hand, in simulations of the SDE, synchrony is defined by the condition $|\Phi| < 10^{-3}$.

3 Partially correlated noise

So far we have considered the effects of a common or fully correlated extrinsic noise source (environmental noise) on the synchronization of a pair of predator–prey oscillators. However, a basic assumption of the above model is that in the absence of environmental noise, each predator–prey patch can be modeled by a deterministic system of ODEs in which the number of predators and prey are treated as

continuous variables. Such an approximation is reasonable when the populations within a patch are sufficiently large. In recent years there has been a growing interest in developing stochastic individual-based descriptions of ecological systems in which explicit rules determining the interaction of individuals are specified (Roos et al. 1991; McCauley et al. 1993; Ghandi et al. 1998, 2000). Under the assumption that the system is well mixed, one can derive deterministic ODE models in the mean-field limit. One of the advantages of individual-based models is that it is also possible to study the effects of demographic noise for finite populations (finite-size effects). One example of such a theory has been developed by McKane and Newman based on a stochastic urn model (McKane and Newman 2004, 2005). In this type of model a single patch is divided into M plots of equal area, with the plot size chosen so that each one contains one prey (species A) or one predator (species B) or neither (an empty plot denoted by E). One then imagines taking all the A, B and E from their particular sites and mixing them together into a single patch in which spatial location is now ignored. The time evolution of the model is then specified as follows: at each time step randomly select either a single individual or a pair of individuals from the population and implement a set of rules associated with the given model. These rules take the form of state transitions with model-dependent transition rates. For example, $A \rightarrow E$ and $AE \rightarrow AA$ represent the death and birth of an individual of species A, respectively, whereas $AB \rightarrow EB$ represents a predator–prey interaction.

Since a stochastic urn model realises a Markov process, it is possible to describe a continuous time version of the model in terms of a master equation (McKane and Newman 2004, 2005; Lai et al. 2011). The latter describes the evolution of the probability $P(m_A, m_B, t)$ that there are $M_A(t) = m_A$ individuals of species A and $M_B(t) = m_B$ individuals of species B within a patch at time t , with the constraint $M_A(t) + M_B(t) + M_E(t) = M$. For large but finite M one can then carry out a system-size expansion familiar from the study of chemical master equations (Van Kampen 1992), in order to approximate the stochastic dynamics in terms of an FP equation. The latter describes the evolution of the PDF of an associated SDE for the stochastic variables $X_A(t) = M_A(t)/M$ and $X_B(t) = M_B(t)/M$ with X_A, X_B treated as continuous variables. The main consequence of such an analysis is that finite size effects generate a source of demographic noise. Of particular significance is that demographic noise is uncorrelated across different patches within a metacommunity. Previously, we have used a stochastic urn model to analyse the combined effects of correlated environmental noise (Moran effect) and uncorrelated demographic noise on the stochastic synchronisation of a population of uncoupled predator–prey oscillators (Lai et al. 2011). As one might expect, the inclusion of uncorrelated noise counteracts the synchronising effects of common environmental noise with the degree of synchronization an increasing function of M . That is, M determines the level of correlations between patches.

In this paper we will consider another mechanism for generating partially correlated noise, namely, a heterogeneous environment. In particular, we will use the model of partial correlations considered by Evans et al. (2012). The Langevin equations (5) now take the form

$$\begin{aligned} \frac{dH_i}{d\tau} &= F_h(\mathbf{X}_i) + D \sum_{j=1}^N C_{ij}(H_j - H_i) + H_i \zeta_i(t) \\ \frac{dR_i}{d\tau} &= F_r(\mathbf{X}_i) + D \sum_{j=1}^N C_{ij}(R_j - R_i) + R_i \zeta_i(t), \end{aligned} \tag{33}$$

where ζ_i is a linear sum of independent white noise processes η_j :

$$\zeta_i = \sum_j \Gamma_{ij} \eta_j. \tag{34}$$

Thus $\langle \zeta_i \rangle = 0$ and

$$\langle \zeta_i \zeta_j \rangle = \sum_k \Gamma_{ik} \Gamma_{jk} = [\mathbf{\Gamma}^T \mathbf{\Gamma}]_{ij} \equiv \mathbf{\Sigma}_{ij}, \tag{35}$$

and $\mathbf{\Sigma}$ can be identified as the correlation matrix. Since the patches are taken to be identical, we set $\Gamma_{ii} = \Gamma_{jj}$ for all i, j . We also assume that $\Gamma_{ij} = \Gamma_{ji}$ (pair-wise symmetry) and that $\langle \zeta_i \zeta_i \rangle = \sum_j \Gamma_{ij}^2 = 1$. Let us now focus on two patches with $i = 1, 2$ and

$$\Gamma_{11}^2 + \Gamma_{12}^2 = \Gamma_{22}^2 + \Gamma_{21}^2 = 1 \tag{36}$$

Our various assumptions regarding $\mathbf{\Gamma}$ allow us to write

$$\Gamma_{11} = \Gamma_{22} =: \gamma \tag{37}$$

$$\Gamma_{12} = \Gamma_{21} = \sqrt{1 - \gamma^2} \tag{38}$$

It follows that the correlation between patches ρ is

$$\rho^2 \equiv \langle \zeta_1, \zeta_2 \rangle = 2\gamma\sqrt{1 - \gamma^2} \tag{39}$$

In other words, to implement a desired level of correlation ρ , the noise is decomposed as

$$\zeta_1 = \gamma \eta_1 + \sqrt{1 - \gamma^2} \eta_2$$

$$\zeta_2 = \sqrt{1 - \gamma^2} \eta_1 + \gamma \eta_2$$

where

$$\gamma = \sqrt{\frac{1 \pm \sqrt{1 - \rho^4}}{2}}. \tag{40}$$

The existence of two solutions for Γ in terms of ρ reflects the fact that

$$\left(\begin{array}{cc} \gamma & \sqrt{1-\gamma^2} \\ \sqrt{1-\gamma^2} & \gamma \end{array} \right), \quad \text{and} \quad \left(\begin{array}{cc} \sqrt{1-\gamma^2} & \gamma \\ \gamma & \sqrt{1-\gamma^2} \end{array} \right)$$

are equivalent, since the independent noise sources η_i are i.i.d. If $\rho = 0$ then $\gamma = 0$ or 1 as expected. In the case of fully correlated noise ($\rho = 1$), $\gamma = \frac{1}{\sqrt{2}}$, meaning that $\zeta_1 = \zeta_2 = \frac{1}{\sqrt{2}}(\eta_1 + \eta_2)$, that is, they are both given by the same Brownian motion.

Without loss of generality we select γ to be the larger root i.e. $\gamma^2 = (1 + \sqrt{1 - \rho^4})/2$ and $1/\sqrt{2} < \gamma < 1$.

Note that an analogous system of equations with partially correlated noise has been studied at some length by Ly and Ermentrout (2009) within the context of a pair of coupled neuronal oscillators. However, these authors were mainly concerned with developing a computationally efficient method for calculating the steady-state PDF based on the use of Fourier methods and asymptotic reduction techniques. They then applied their phase reduction method to study the behavior of a realistic synaptically-coupled system of Morris–Lecar oscillators. One of their main results was to show that the combination of weak coupling and partially correlated noise can lead to bistability (in the probabilistic sense) between a synchronous and an asynchronous state. An analogous result will hold in the case of our population model.

We now proceed along identical lines to Sect. 2. That is, applying the phase reduction method ultimately leads to the following Stratonovich SDE for the stochastic phases:

$$d\Theta_i = \left(\omega + D\mathbf{Z} \cdot \mathbf{R} - \frac{\sigma^2 \gamma^2}{2} \alpha - \frac{\sigma^2 (1 - \gamma^2)}{2} \alpha \right) dt + \sigma \alpha \left(\gamma dW_i + \left(\sqrt{1 - \gamma^2} \right) dW_j \right), \tag{41}$$

where $dW_i(t) = \xi_i(t)dt$ and $i = 1, 2, j = 2, 1$. Here α and \mathbf{R} are given by Eqs. (12) and (16) respectively. It can be seen that changing the noise to be partially correlated does not affect the drift terms. Hence we can write our ensemble in the Ito formulation as

$$d\Theta_i = \mathcal{A}_i(\Theta) + d\xi_i(\Theta, t) \tag{42}$$

where \mathcal{A}_i is the same as before but our noise terms are

$$d\xi_i = \sigma \left[\alpha(\Theta_i) \gamma dW_i + \alpha(\Theta_j) \sqrt{1 - \gamma^2} dW_j \right]. \tag{43}$$

Hence if we define a new correlation matrix

$$\langle d\xi_i d\xi_j \rangle = \Delta_{ij}^* dt \tag{44}$$

we have

$$\Delta_{ii}^* = \sigma^2 \alpha(\Theta_i)^2 \tag{45}$$

$$\Delta_{ij}^* = 2\sigma^2 \gamma \sqrt{1 - \gamma^2} \alpha(\Theta_i) \alpha(\Theta_j) = \sigma^2 \rho^2 \alpha(\Theta_i) \alpha(\Theta_j), i \neq j \tag{46}$$

or, more compactly,

$$\Delta_{ij}^* = \sigma^2 (\rho^2 + (1 - \rho^2) \delta_{i,j}) \alpha(\Theta_i) \alpha(\Theta_j) \tag{47}$$

Averaging as in the case of fully correlated noise generates the same effective drift term \bar{A} , equation (19), while

$$\bar{\Delta}_{ij}^* = \sigma^2 (\rho^2 \Delta(\psi_j - \psi_i) + (1 - \rho^2) \Delta(0)) \tag{48}$$

with the function Δ defined in equation (22).

As in Sect. 2, we introduce the phase difference Φ to obtain

$$d\psi_1 = D\mathcal{H}(\Phi)dt + d\bar{\zeta}_1(\Phi, t) \tag{49}$$

$$d\psi_2 = D\mathcal{H}(-\Phi)dt + d\bar{\zeta}_2(\Phi, t), \tag{50}$$

with

$$\begin{aligned} \langle d\bar{\zeta}_1(\Phi, t) d\bar{\zeta}_1(\Phi, t) \rangle &= \langle d\bar{\zeta}_2(\Phi, t) d\bar{\zeta}_2(\Phi, t) \rangle = \sigma^2 \Delta(0) \\ \langle d\bar{\zeta}_1(\Phi, t) d\bar{\zeta}_2(\Phi, t) \rangle &= \langle d\bar{\zeta}_2(\Phi, t) d\bar{\zeta}_1(\Phi, t) \rangle = \sigma^2 \rho^2 \Delta(\Phi) \end{aligned} \tag{51}$$

Taking the difference of the equations and using the result that the difference of two Gaussian random variables is also Gaussian leads to the scalar SDE

$$d\Phi = DG(\Phi)dt + \sigma K^*(\Phi)dW(t), \tag{52}$$

where $G(\phi) = H(\phi) - H(-\phi)$ is the odd part of the phase interaction function H , $W(t)$ is a Wiener process and

$$\begin{aligned} K^*(\Phi) &= \frac{1}{\sigma} \sqrt{\langle [d\bar{\zeta}_2(\Phi, t) - d\bar{\zeta}_1(\Phi, t)][d\bar{\zeta}_2(\Phi, t) - d\bar{\zeta}_1(\Phi, t)] \rangle} \\ &= \sqrt{2[\Delta(0) - \rho^2 \Delta(\Phi)]}. \end{aligned} \tag{53}$$

Therefore we can derive an FPE and solve for a stationary distribution P_0 as in Sect. 2:

$$\frac{\partial P(\phi, t)}{\partial t} = -D \frac{\partial}{\partial \phi} G(\phi) P(\phi, t) + \frac{\sigma^2}{2} \frac{\partial^2}{\partial \phi^2} K^*(\phi)^2 P(\phi, t). \tag{54}$$

and

$$P_0(\phi) = \frac{A}{\Delta(0) - \rho^2 \Delta(\phi)} \exp\left(\int_0^\phi \frac{DG(s)ds}{\sigma^2(\Delta(0) - \rho^2 \Delta(s))}\right) \tag{55}$$

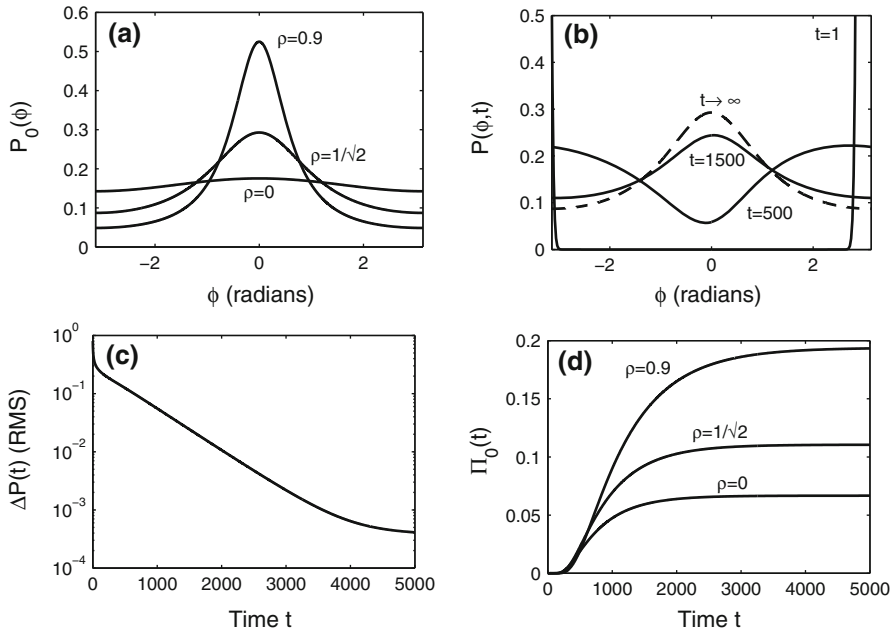


Fig. 7 Monostable case with partially correlated noise. All parameters except ρ are the same as Fig. 4. **a** Steady-state PDFs for various values of ρ . **b** For $\rho = 1/\sqrt{2}$, the PDF is plotted at several points in time, starting from the initial condition $\phi_0 = 3$ radians. **c** Plot of root-mean-square difference between the numerical solution to the Fokker–Planck equation and the analytical steady-state solution, $\Delta P(t) = \sqrt{\int_0^{2\pi} [p(\phi, t) - P_0(\phi)]^2 d\phi}$, as a function of time with $\rho = 1/\sqrt{2}$. **d** Plot of $\Pi_0(t) = \int_{-0.2}^{0.2} p(\phi, t) d\phi$ against time for various values of ρ

Note that $\rho = 1$ recovers the case of fully correlated noise, see Eq. (32), whereas $\rho = 0$ (uncorrelated noise) means that our stationary distribution is only dependent on the G -function, with peaks at zero as expected.

We now explore the effects of partially correlated noise on synchronisation by numerically solving the FP equation (54). In the monostable case, see Fig. 7, where both dispersal and common environmental noise cause the system to synchronize irrespective of initial conditions, reducing the level of correlation simply broadens the steady-state PDF to give a unimodal function centred at $\phi = 0$ whose width increases as the level of correlation ρ decreases. In the multistable case, introducing a small amount of decorrelation ($\rho = 0.99$) leads to a PDF with multiple peaks at intermediate times before converging to a unimodal steady-state centred about $\phi = 0$, see Fig. 8a–c. Reducing the level of correlated noise ($\rho = 0.9$) causes the transient peaks to persist so that the steady-state PDF develops multiple peaks indicative of a stochastic bifurcation, see Fig. 9a, b. Finally, for low levels of correlated noise the steady-state PDF approaches a uniform distribution around the synchronous state, see Fig. 9c, d. It is also instructive to see how the steady-state probability of being in a neighborhood of the synchronous state $\phi = 0$ or the asynchronous state $\phi = \phi_a = 1.78$ varies with ρ and σ . Thus let $\Pi_\phi = \int_{\phi-\Delta}^{\phi+\Delta} P_0(\phi') d\phi'$ with $\Delta = 0.2$ be a measure of the degree of stochastic phase-locking around the phase ϕ . In Fig. 10 we plot Π_0 and

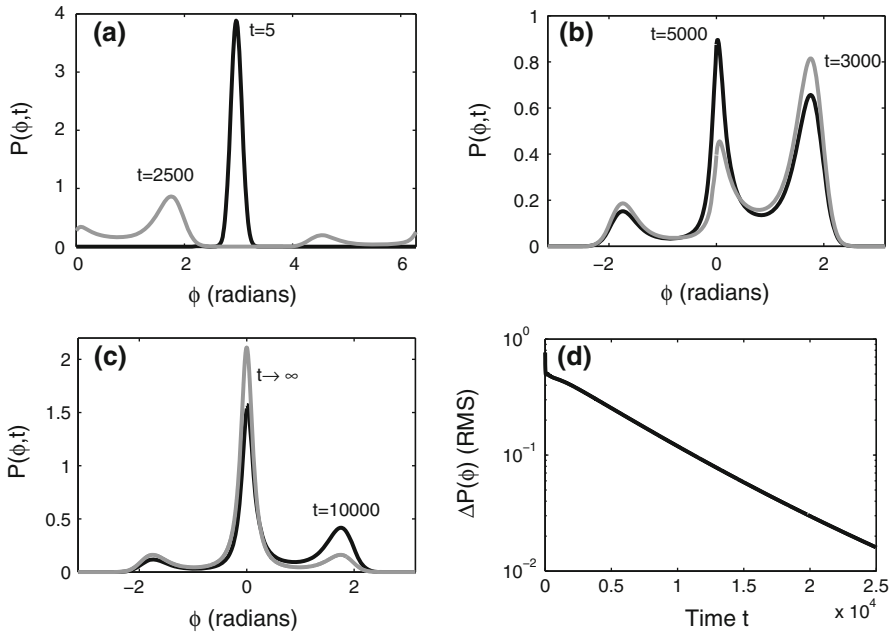


Fig. 8 Multistable case with very high correlations ($\rho = 0.99$). All other parameters are the same as Fig. 5. **a–c** Snapshots of the PDF $P(\phi, t)$ with $P(\phi, 0) = \delta(\phi - \phi_0)$ and $\phi_0 = 3$. **a** At relatively short times the PDF develops two peaks at the deterministic asynchronous states $\phi \approx 1.78$ and $2\pi - 1.78$. **b** At intermediate times the PDF develops a third peak at $\phi = 0$. **c** At longer times the PDF approaches the steady-state solution which is given by a single peak centered about the synchronous state. **d** Plot of root-mean-square $\Delta P(t)$ as a function of time with $\rho = 1/\sqrt{2}$

$\Pi_a + \Pi_{-a}$ as a function of the noise level σ and correlation ρ . It can be seen that when the noise source is highly correlated and sufficiently strong ($\sigma > 10^{-4}$, $\rho \approx 1$) there is a high probability that the oscillators are approximately synchronized with $\Pi_0 \approx 1$ and $\Pi_a \approx 0$. As the level of correlation ρ is decreased for fixed σ , the degree of synchronization decreases but there is still a low probability of being in the asynchronous states. On the other hand, for sufficiently weak noise ($\sigma < 10^{-4}$), the oscillators occupy one of the two asynchronous states with a probability $\Pi_a \approx 0.5$, and this is insensitive to the level of correlated noise. Interestingly, there is a sharp transition between synchrony and asynchrony as σ increases for fixed ρ .

4 Discussion

In this paper we used the theory of noise-induced phase synchronization to analyze the effects of dispersal on the synchronization of a pair of predator–prey systems within a fluctuating environment. We first showed that in the case of common environmental noise, the oscillators ultimately synchronize. However, the approach to synchrony depends on whether or not there exist stable asynchronous states in the deterministic limit. We found that in the absence of asynchronous states, the time-dependent PDF was unimodal with a width that first increased and then decreased as it moved

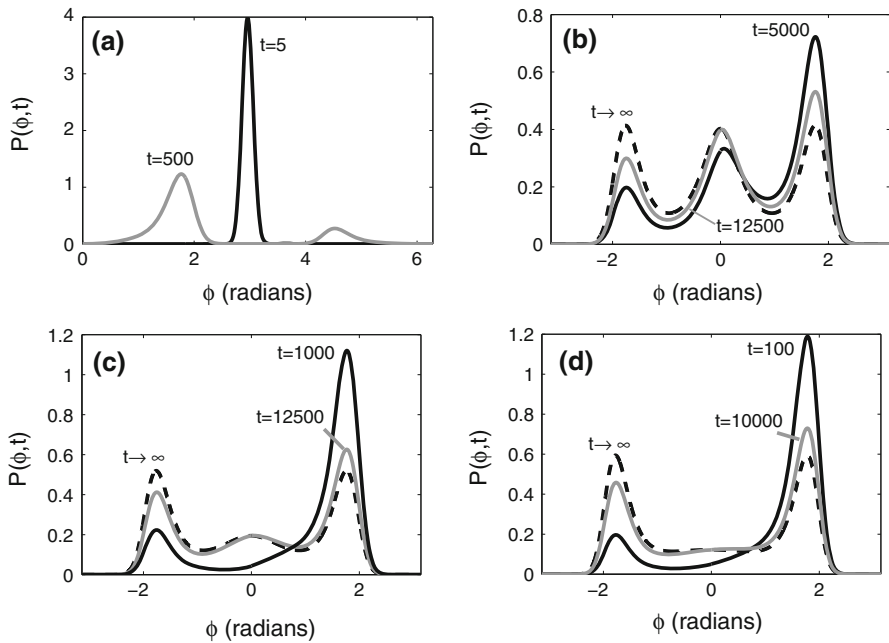


Fig. 9 **a, b** Same as Fig. 8 for a lower level of correlated noise ($\rho = 0.9$). The PDF is plotted at various points in time to show the emergence of persistent peaks around the asynchronous states and convergence to a multistable steady state. **c, d** Low levels of correlated noise ($\rho = 1/\sqrt{2}, 0$), the steady-state distribution becomes more uniform around the synchronous state

towards the synchronous state. Moreover, the rate of stochastic synchronization varied approximately linearly with the initial phase difference between the two oscillators. On the other hand, if dispersal also supported asynchronous phase-locking, then the corresponding PDF exhibited a broad bimodal structure at intermediate times before ultimately converging to the synchronous state. This led to a sharp decrease in the rate of stochastic synchronisation as the initial phase difference increased from zero. We then investigated how these two distinct scenarios were affected by partially correlated noise. In particular, we showed how reducing the level of correlation can cause the transient peaks in the PDF associated with asynchronous states to become persistent, resulting in a multimodal steady-state PDF that is indicative of a stochastic bifurcation.

One obvious extension of our work would be to consider a metapopulation of $N > 2$ predator–prey oscillators with both dispersal and noise. This is a considerably more involved problem from an analytical perspective. Following previous studies of the Kuramoto model (Kuramoto 1984; Strogatz 2000), one could proceed by identifying appropriate macroscopic variables (for large N) that characterize the degree of synchrony of the system. A common choice is the complex amplitude defined according to

$$Re^{i\psi} = \frac{1}{N} \sum_{i=1}^N e^{i\theta_i}.$$

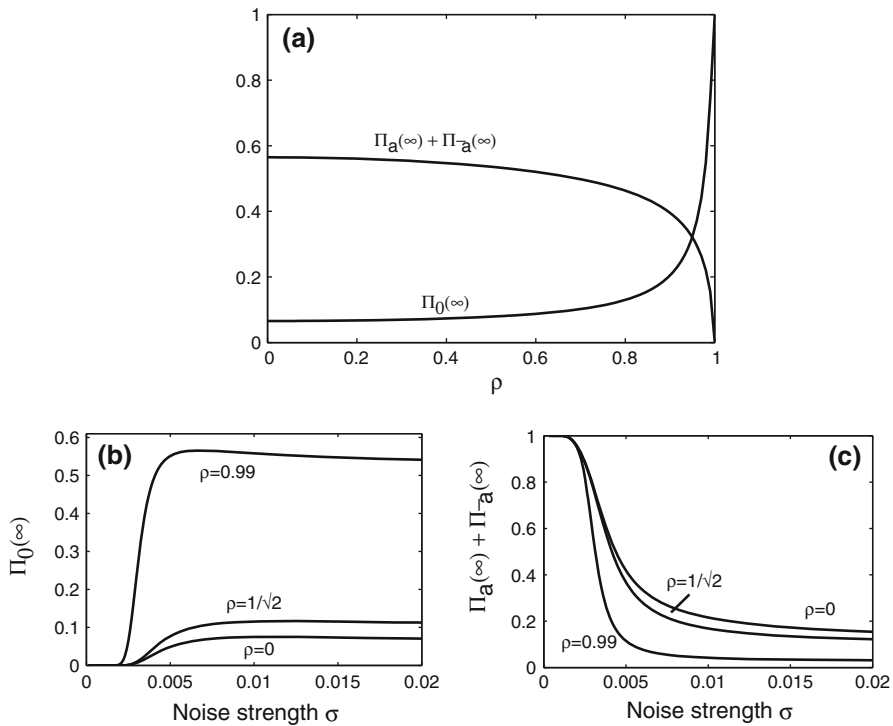


Fig. 10 **a** Plots of probability of being in the synchronous (Π_0) or an asynchronous state ($\Pi_a + \Pi_{-a}$) against the correlation ρ for fixed $\sigma = 5 \times 10^{-3}$. **b** Plot of Π_0 against noise strength σ for various ρ ; **c** Plot of $\Pi_a + \Pi_{-a}$ against noise strength σ for various ρ

The amplitude $R \in [0, 1]$ with $R = 1$ denoting complete synchrony and $R = 0$ denoting complete asynchrony. In the case of common noise and dispersal, we expect the population to converge to a synchronous state just as for a pair of oscillators. One could then investigate numerically how the approach to synchrony ($R(t) \rightarrow 1$ as $t \rightarrow \infty$) depends on the initial distribution of phases and the various phase-locked states in the deterministic limit. For large N there could be a large number of such states associated with various forms of clustering. Including the effects of intrinsic noise would counter the synchronizing effects of dispersal and common noise, but characterizing the associated steady-state PDF for N phases would be non-trivial.

Another extension of our work would be to carry out a comparison between different sources of partially correlated noise, namely, heterogeneous environmental noise and intrinsic demographic noise (due to finite-size effects). The latter is uncorrelated across different patches within a metacommunity so that under a Langevin approximation it leads to an additional multiplicative noise term which, when combined with a common environmental noise source, results in partially correlated noise (Lai et al. 2011). The degree of correlation increases with the size of the populations. One major difference is that fluctuations due to intrinsic noise typically depend nonlinearly on the size of the populations rather than the linear dependence assumed for environmental noise.

Our results could provide an analytical framework for interpreting various ecological experiments to determine the dominant factors behind the behaviour of ecosystems - for example, controlled experiments could be done in phytoplankton-zooplankton systems, with different levels of environmental fluctuations and ease of dispersal between populations, that could be compared with our results to find out which parameter regime the system is in. In the field, population data could be processed in a similar manner - for instance, constant time-lags between the peaks of populations of adjacent patches would be indicative of a constant phase difference, showing that the asynchronous dispersal-induced state was present; alternatively, switching between this constant delay and synchronization would demonstrate multistability.

Acknowledgments This publication was based on work supported in part by the National Science Foundation (DMS-1120327) and the King Abdullah University of Science and Technology Award No. KUK-C1-013-04.

References

- Bressloff PC, Lai YM (2011) Stochastic synchronization of neuronal populations with intrinsic and extrinsic noise. *J Math Neurosci* 1:2
- Colombo A, Dercole F, Rinaldi S (2008) Remarks on metacommunity synchronization with application to prey-predator systems. *Am Nat* 171:430-442
- Earn DJD, Rohani P, Grenfell BT (1998) Persistence, chaos and synchrony in ecology and epidemiology. *Proc R Soc Lond Ser B Biol Sci* 265:7-10
- Ermentrout GB, Kopell N (1991) Multiple pulse interactions and averaging in coupled neural oscillators. *J Math Biol* 29:195-217
- Evans SN, Ralph PL, Schreiber SJ, Sen A (2012) Stochastic population growth in spatially heterogeneous environments. *J Math Biol* (published online)
- Galan RF, Ermentrout GB, Urban NN (2006) Correlation-induced synchronization of oscillations in olfactory bulb neurons. *J Neurosci* 26:3646-3655
- Galan RF, Ermentrout GB, Urban NN (2008) Optimal time scale for spike-time reliability: theory, simulations and experiments. *J Neurophysiol* 99:277-283
- Gardiner CW (2009) *Stochastic methods: a handbook for the natural and social sciences*, 4th edn. Springer, New York
- Ghandi A, Levin S, Orszag S (1998) 'Critical slowing down' in time-to-extinction: an example of critical phenomena in ecology. *J Theor Biol* 192:363-376
- Ghandi A, Levin S, Orszag S (2000) Moment expansions in spatial ecological models and moment closure through Gaussian approximation. *Bull Math Biol* 62:595-632
- Goldobin DS, Pikovsky A (2005) Synchronization and desynchronization of self-sustained oscillators by common noise. *Phys Rev E* 71:045201
- Goldwyn EE, Hastings A (2008) When can dispersal synchronize populations? *Theor Popul Biol* 73:395-402
- Goldwyn EE, Hastings A (2009) Small heterogeneity has large effects on synchronisation of ecological oscillators. *Bull Math Biol* 71:130-144
- Goldwyn EE, Hastings A (2011) The roles of the Moran effect and dispersal in synchronizing oscillating populations. *J Theor Biol* 289:237-246
- Hanski I (1998) *Metapopulation dynamics*. Nature 396:41-49
- Hastings A (1997) *Population biology: concepts and models*. Springer, New York
- Hudson PJ, Cattadori IM (1999) The Moran effect: a cause of population synchrony. *Trends Ecol Evol* 14:1-2
- Jansen VAA, Lloyd AL (2000) Local stability analysis of spatially homogeneous solutions of multi-patch systems. *J Math Biol* 41:232-252
- Klausmeier CA (2010) Successional state dynamics: a novel approach to modeling nonequilibrium foodweb dynamics. *J Theor Biol* 262:585-595

- Kuramoto Y (1984) *Chemical oscillations, waves and turbulence*. Springer, Berlin
- Lai YM, Newby J, Bressloff PC (2011) Effects of demographic noise on the synchronization of metacommunities by a fluctuating environment. *Phys Rev Lett* 107:118102
- Liebhold A, Koenig WD, Bjornstad ON (2004) Spatial synchrony in population dynamics. *Annu Rev Ecol Evol Syst* 35:467–490
- Ly C, Ermentrout GB (2009) Synchronization of two coupled neural oscillators receiving shared and unshared noisy stimuli. *J Comput Neurosci* 26:425–443
- Mainen ZF, Sejnowski TJ (1995) Reliability of spike timing in neocortical neurons. *Science* 268:1503–1506
- Marella S, Ermentrout GB (2008) Class-II neurons display a higher degree of stochastic synchronization than class-I neurons. *Phys Rev E* 77:41918
- McCauley E, Wilson WG, Roos AM (1993) Dynamics of age-structured predator–prey interactions: individual based models and population level formulations. *Am Nat* 142:412–442
- McKane AJ, Newman TJ (2004) Stochastic models in population biology and their deterministic analogs. *Phys Rev E* 70:041902
- McKane AJ, Newman TJ (2005) Predator–prey cycles from resonant amplification of demographic stochasticity. *Phys Rev Lett* 94:218102
- Moran PAP (1953) The statistical analysis of the Canadian lynx cycle. II. Synchronisation and meteorology. *Aust J Zool* 1:291–298
- Nakao H, Arai K, Kawamura Y (2007) Noise-induced synchronization and clustering in ensembles of uncoupled limit cycle oscillators. *Phys Rev Lett* 98:184101
- Oksendal B (2000) *Stochastic differential equations: an introduction with applications*. Springer, Berlin
- Pecora LM, Carroll TL (1998) Master stability functions for synchronized coupled systems. *Phys Rev Lett* 80:2109–2112
- Pikovsky AS (1984) Synchronization and stochastization of an ensemble of autogenerators by external noise. *Radiophysics* 27:576–581
- Renshaw E (1993) *Modelling biological populations in space and time*. Cambridge University Press, Cambridge
- Rohani P, Earn DJD, Grenfell BT (1999) Opposite patterns of synchrony in sympatric disease metapopulations. *Science* 286:968–971
- Roos AM, McCauley E, Wilson WG (1991) Mobility versus density-limited predator–prey dynamics on different spatial scales. *Proc R Soc Lond B* 246:117–122
- Rosenzweig ML, MacArthur RH (1963) Graphical representation and stability conditions of predator–prey interactions. *Am Nat* 97:209–223
- Strogatz SH (2000) From Kuramoto to Crawford: exploring the onset of synchronization in populations of coupled oscillators. *Physica D* 143:1–20
- Teramae JN, Tanaka D (2004) Robustness of the noise-induced phase synchronization in a general class of limit cycle oscillators. *Phys Rev Lett* 93:204103
- Teramae JN, Nakao H, Ermentrout GB (2009) Stochastic phase reduction for a general class of noisy limit cycle oscillators. *Phys Rev Lett* 102:194102
- Turelli M (1978) Random environments and stochastic calculus. *Theor Popul Biol* 12:140–178
- Van Kampen NG (1992) *Stochastic processes in physics and chemistry*. North-Holland, Amsterdam
- Vasseur DA, Fox JW (2009) Phase-locking and environmental fluctuations generate synchrony in a predator–prey community. *Nature* 460:1007–1010
- Yoshimura K, Arai K (2008) Phase reduction of stochastic limit cycle oscillators. *Phys Rev Lett* 101:154101